Soft Matter

Colloidal Stability versus Self-Assembly of Nanoparticles Controlled by Coiled-Coil Protein Interactions

Journal:	*Soft Matter*
Manuscript ID	SM-COM-07-2019-001314.R1
Article Type:	Communication
Date Submitted by the Author:	22-Aug-2019
Complete List of Authors:	Siehr, Allison; University of Minnesota Twin Cities, Biomedical Engineering Xu, Bin; University of Minnesota Twin Cities, Biomedical Engineering Siegel, Ronald; University of Minnesota, Department of Pharmaceutics Shen, Wei; University of Minnesota,

COMMUNICATION

Colloidal Stability versus Self-Assembly of Nanoparticles Controlled by Coiled-Coil Protein Interactions

Allison Siehr,[a] Bin Xu,[a] Ronald A. Siegel*[a,b] and Wei Shen*[a]

Received 00th January 20xx,
Accepted 00th January 20xx

DOI: 10.1039/x0xx00000x

Orientational discrimination of biomolecular recognition is exploited here as a molecular engineering tool to regulate nanoparticle self-assembly or stability. Nanoparticles are conjugated with the heterodimerizing coiled-coils, A and B, which associate in parallel orientation. Simply flipping the orientation of one coiled-coil results in either self-assembling or colloidally stable nanoparticles.

Controlled nanoparticle self-assembly or stability is essential for technological development in nanomedicine and nanobiotechnology.[1,2] For example, nanoparticles used for computerized tomography imaging and plasmonic photothermal therapies are required to be highly stable under physiological conditions.[3,4] Controlled nanoparticle self-assembly has been extensively exploited to develop therapeutic methods for viral inhibition and detection technologies for biomolecules, viruses, and circulating tumor cells.[5–10]

Currently, the most common approach to stabilize nanoparticles is surface modification with poly(ethylene glycol) (PEG),[11–13] although approaches using zwitterionic ligands have also been proposed.[14] Self-assembly of nanoparticles into larger hierarchical structures is typically engineered on the basis of hydrophobic interactions, electrostatic interactions, and biomolecular recognition.[15–20] Biomolecular recognition modes, such as DNA hybridization,[21–23] coiled-coil self-assembly,[24–26] streptavidin-biotin interactions,[27] and antibody-antigen interactions,[28] have high specificity, and have been extensively used to direct nanoparticle self-assembly. Hybridization of DNA complementary strands and self-assembly of some protein domains, such as coiled-coils, exhibit orientational discrimination,[29] making these modes more versatile in controlling self-assembly and forming nanoparticle superstructures.

Here we report that orientational discrimination of biomolecular recognition can be used as a molecular tool to control nanoparticle self-assembly and stability. In a model system, we conjugated a pair of heterodimerizing coiled-coil proteins, "A" and "B",[30] on gold nanoparticles (GNPs). While the A protein was conjugated to the GNPs in a fixed orientation, the B protein was conjugated at either its N-terminal or C-terminal side, providing two different orientations of this domain on the particle surface. Simply flipping the orientation of B led to two completely different particle behaviors: one orientation maintaining colloidal stability of the GNPs, and the other orientation driving GNPs into large aggregates.

The molecular design of the nanoparticles is illustrated in Figure 1. A and B proteins have been previously shown to heterodimerize in the parallel direction through hydrophobic and electrostatic interactions.[30] Immobilizing A and B in anti-parallel orientation on the same nanoparticle results in a parallel orientation on adjacent nanoparticles, promoting interparticle protein heterodimerization and nanoparticle self-assembly (Fig. 1a). Alternatively, intraparticle protein heterodimers can form when A and B are immobilized in parallel orientation on the same nanoparticle. These coiled-coils do not bridge adjacent nanoparticles, resulting in colloidal stability (Fig. 1b).

GNPs synthesized using the Frens-Turkevich method were characterized by dynamic light scattering (DLS) and UV-Vis spectrophotometry.[31] DLS revealed a hydrodynamic diameter of 20.5±0.7 nm with a polydispersity of 0.077±0.020. The UV-Vis spectrum showed a characteristic maximum absorbance at 518 nm, corresponding to surface plasmon resonance (SPR) of GNPs having a diameter of 16.8 nm.[32,33] The GNP concentration was determined by the ratio of the absorbance at the SPR peak to that at 450 nm as previously reported (see ESI for detailed information).[33]

Two non-cysteinated coiled-coil proteins, nA and nB, and three cysteinated coiled-coil proteins, cysA, cysB, and Bcys, were synthesized (see Table S1 for protein sequences, ESI). In the cysteinated proteins, the cysteine residue was incorporated near the N-terminus of the coiled-coil domain in cysB and cysA, and near the C-terminus in Bcys.

By combining heterodimers of a non-cysteinated protein with its cysteinated partner, solutions were prepared

[a] Department of Biomedical Engineering, University of Minnesota, 312 Church St. SE, 7-105 Nils Hasselmo Hall, Minneapolis, Minnesota 55455. E-mail: shenx104@umn.edu, Tel: 612-624-3378
[b] Department of Pharmaceutics, University of Minnesota, 308 SE Harvard St, Room 9-177 Weaver Densford Hall, Minneapolis, Minnesota 55455. E-mail: siege017@umn.edu, Tel: 612-624-6164
Electronic Supplementary Information (ESI) available. See DOI: 10.1039/x0xx00000x

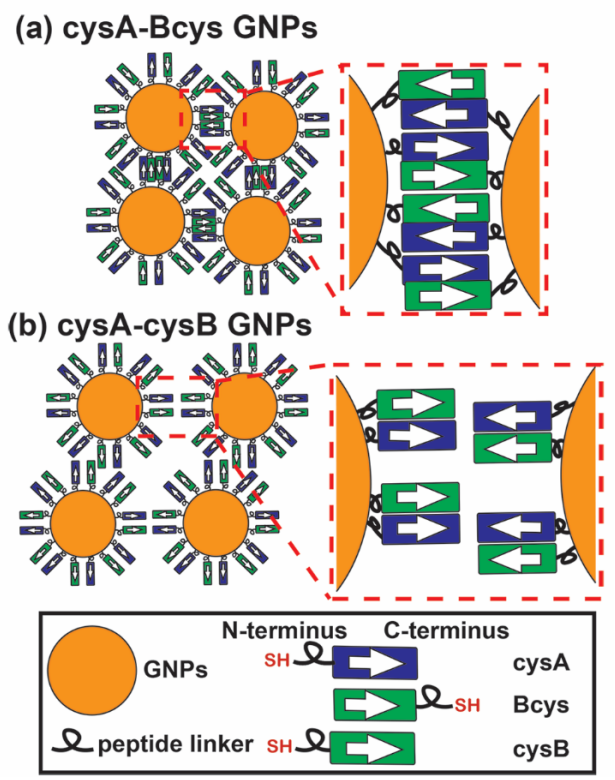

Figure 1 The molecular design of the nanoparticles. (a) When coiled-coils A and B are conjugated on nanoparticles in anti-parallel orientation, A and B on adjacent particles are parallel and form interparticle heterodimers that promote nanoparticle self-assembly. (b) When coiled-coils A and B are conjugated on nanoparticles in parallel orientation, A and B on the same particle form intraparticle heterodimers, and the nanoparticles remain colloidally stable.

containing nA and cysB (nA/cysB), nA and Bcys (nA/Bcys), and cysA and nB (cysA/nB) in the presence of a reducing agent, tris(2-carboxyethyl)phosphine (TCEP) (75 μM and 50 μM for non-cysteinated and cysteinated proteins, respectively). These heterodimers were then conjugated to the GNPs by gold-thiol reaction. Specifically, the solutions of nA/Bcys and cysA/nB or the solutions of nA/cysB and cysA/nB were mixed at a 1:1 ratio, and the mixture was added to a GNP suspension (1.53×10^{12} GNPs mL^{-1}) at a 1:3 ratio while stirring. Solutions of coiled-coil protein heterodimers, in which one partner was non-cysteinated, were used in order to prevent an excessively dense packing of covalently conjugated proteins, which may inhibit interparticle coiled-coil heterodimerization. The GNPs modified with cysA and Bcys (denoted here as cysA-Bcys GNPs) had the two coiled-coils conjugated on the surface in anti-parallel orientation, and the GNPs modified with cysA and cysB (denoted as cysA-cysB GNPs) had the two coiled-coils on the surface in parallel orientation (Fig. 1).

Table 1 The properties of unmodified and protein conjugated GNPs characterized with DLS and UV-Vis spectrophotometry.

	Dynamic Light Scattering		*UV-Vis spectrophotometry*
Sample	**Size (nm)**	**Polydispersity**	**Maximum SPR (nm)**
Unmodified GNPs	20.5±0.7	0.077±0.02	518
cysA-Bcys GNPs	35.2±0.4	0.069±0.018	524
cysA-cysB GNPs	35.7±0.4	0.077±0.009	524

Immediately following protein conjugation, DLS revealed hydrodynamic diameters of approximately 35 nm for both cysA-Bcys and cysA-cysB conjugated GNPs (Table 1). The change in hydrodynamic diameter from 20 nm for unmodified GNPs to 35 nm for coiled-coil conjugated GNPs suggests an approximately 7.5 nm thick corona. This is largely consistent with the 6.3 nm length of the coiled-coil rods as previously reported[34] plus the additional small linker sequence length of ~1.6 nm (see SAXS data below for further information). The polydispersity of the protein conjugated GNPs was the same as that of unmodified GNPs, suggesting that aggregation did not occur during or after the conjugation procedure. Colloidal stability of GNPs at this step was most likely maintained by the large excess of unbound coiled-coils in the solution, which dominated strand exchange with the noncovalently immobilized coiled-coils on the GNPs and prevented interparticle coiled-coil interactions. The protein conjugated GNPs were also characterized using UV-Vis spectrophotometry. The maximum SPR peak of the UV-Vis spectra shifted from 518 nm for unmodified GNPs to 524 nm for both cysA-Bcys and cysA-cysB conjugated GNPs (Fig. S1, ESI) (Table 1). The red shift in the SPR peak was due to the presence of proteins bound to the GNP surface and suggests that surface modification had occurred.[32]

Nanoparticle behavior after reducing the concentration of unbound coiled-coils in solution was then examined. Specifically, each suspension was centrifuged, and 85% of the supernatant was removed, followed by resuspension in PBS at 50% of the starting suspension volume. The samples were then examined over a time course of 10 days to observe the behavior of the protein conjugated GNPs. The difference between the two types of protein conjugated GNPs was first observed visually (Fig. 2a). On day 0, both suspensions of protein conjugated GNPs appeared red, as expected for non-aggregated GNPs.[32] On day 10, visible dark red and purple aggregates in a clear background were observed for the cysA-Bcys conjugated GNPs, but no visible aggregates or color change was observed for the cysA-cysB conjugated GNPs. Representative UV-Vis spectra of cysA-Bcys conjugated GNPs also exhibited a red-shift and broadening of the SPR peak over 10 days, while those of cysA-cysB conjugated GNPs remained almost unchanged (Fig. 2b). It has been reported that a red-shift in the SPR peak of the UV-vis spectra occurs when GNPs form aggregates.[32,33,35–37] The differences in the UV-Vis spectra between the two particle samples confirm that the cysA-Bcys conjugated GNPs aggregated readily and the cysA-cysB conjugated GNPs were highly stable. As a final confirmation of disparate aggregation behaviors, TEM images (Fig. 3) revealed that the cysA-Bcys conjugated GNPs formed large aggregates after 5 days, while the cysA-cysB conjugated GNPs did not form aggregates at 5 or 10 days.

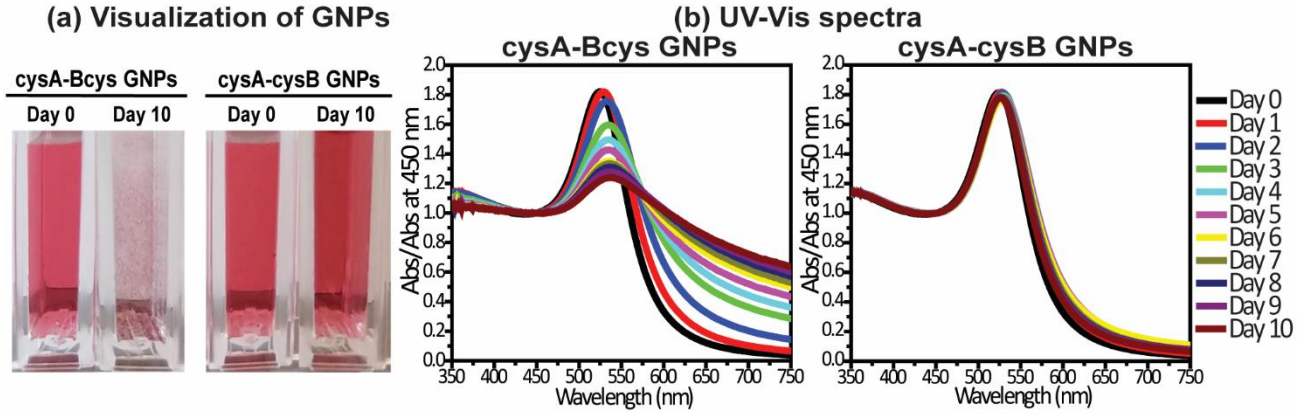

Figure 2 (a) The suspension of cysA-Bcys conjugated GNPs exhibited visible large aggregates on day 10, while the suspension of cysA-cysB conjugated GNPs did not show any visible changes. (b) UV-Vis spectra of protein conjugated GNPs over a time course of 10 days. The spectra of cysA-Bcys conjugated GNPs showed a broadening and a red-shift in the maximum SPR peak over time (left). The spectra of cysA-cysB conjugated GNPs remained almost unchanged (right). All spectra are normalized to the absorbance at 450 nm.

The structure of cysA-Bcys conjugated GNP aggregates was probed using Small Angle X-Ray Scattering (SAXS). SAXS spectra on day 10 (Fig. 4) exhibited a maximum peak at a q-value of 0.234 nm^{-1} for cysA-Bcys conjugated GNPs corresponding to a d-spacing of 26.8 nm (Equation S3, ESI).[38,39] SAXS spectra for cysA-cysB conjugated GNPs were of low amplitude and did not exhibit any distinct peaks on day 10 (Fig. 4). Size of the unmodified GNPs was also characterized using SAXS. Fitting the scattering data to the Guinier function (Fig. S2, ESI) yielded a radius of gyration (R_g) of 6.66±0.11 nm, corresponding to a hard sphere radius of 8.60 nm (Equation S4 and S5, ESI) and a diameter of 17.2 nm, which lies between the previous estimates of particle diameter derived from DLS (20.5 nm) and SPR (16.8 nm). The particle center-to-center distance of 26.8 nm and the particle radius of 8.60 nm suggest that the surface-to-surface distance between neighboring particles was 9.6 nm. This value is largely consistent with that expected for GNP aggregates mediated by interparticle coiled-coil heterodimerization, because these coiled-coil A and B rods are 6.3 nm long[34] and both cysA and Bcys contain a few amino acid residues between cysteine and the coiled-coil domains (suggesting a linker length of 1.6 nm).

To demonstrate that self-assembly of cysA-Bcys conjugated GNPs was due to protein-protein interactions, GNPs self-assembled for 10 days were treated at 80°C to denature the proteins. The UV-Vis spectrum of the resulting GNP suspension was substantially different from that of the aggregated GNPs on day 10, but essentially indistinguishable from that of the pre-aggregation suspension on day 0 (Fig. S3a, ESI), indicating that the self-assembled GNPs could be disassembled upon protein denaturation. The same treatment had no effect on the colloidal stability of cysA-cysB conjugated GNPs (Fig. S3b, ESI).

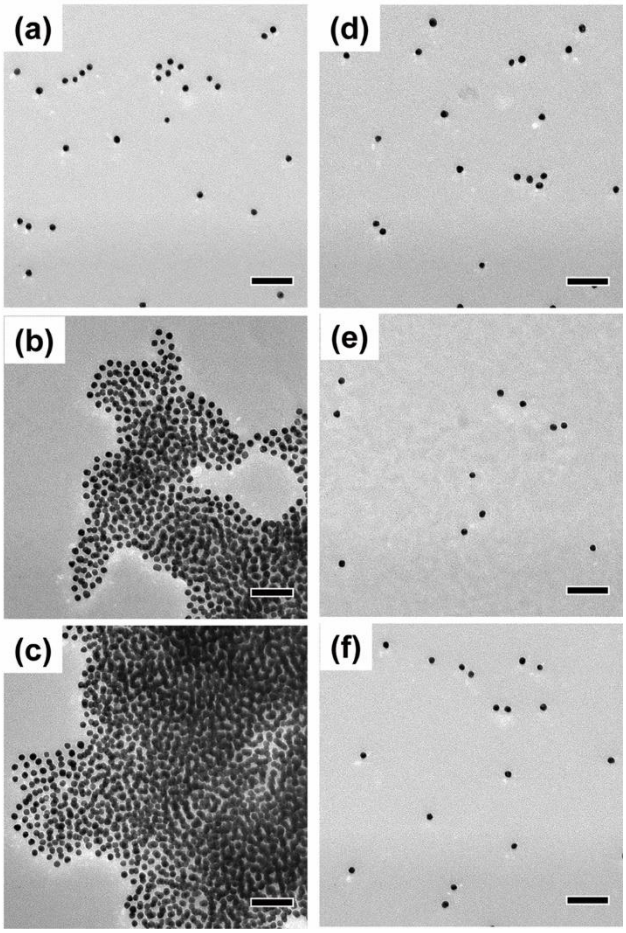

Figure 3 TEM images of cysA-Bcys GNPs (a-c) and cysA-cysB GNPs (d-f) on day 0 (a, d), day 5 (b, e), and day 10 (c, f). Scale bar is 100 nm.

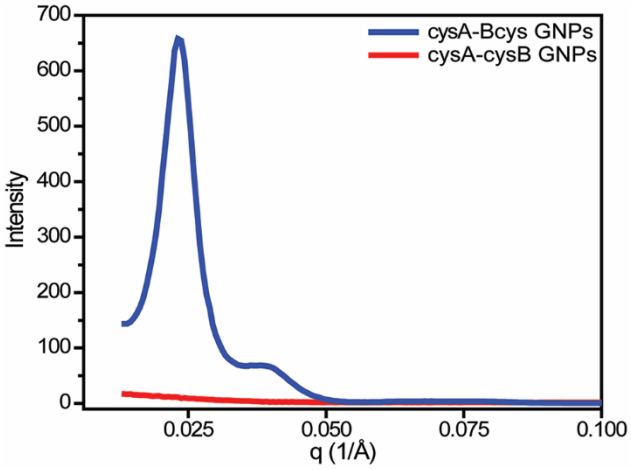

Figure 4 The SAXS profiles for cysA-Bcys and cysA-cysB conjugated GNPs on day 10. The maximum peak in the spectrum of cysA-Bcys conjugated GNPs revealed a d-spacing (center-to-center distance) of 26.8 nm in the aggregates as calculated by $d = 2\pi/q$, where d is the d-spacing and q is the scattering vector.

The inclusion of non-cysteinated partners when the GNPs were conjugated with cysA and Bcys was necessary to provide an optimal spacing between the latter coiled proteins, such that they could form interparticle coiled-coil heterodimers. In the absence of nA and nB, the packing density of cysA and Bcys was too high to permit cysA-Bcys coiled-coil bridges between GNPs, and hence impaired GNP aggregation (Fig. S4, ESI). On the other hand, reducing the packing density of cysA-cysB by conjugating these proteins in the presence of β-mercaptoethanol, a small thiolate that competes with thiol-mediated protein binding to the GNP surface, eliminated GNP colloidal stability (promoted aggregation: Fig. S5, ESI), most likely due to the increased distance between cysA and cysB conjugates, and hence prevention of intraparticle cysA-cysB heterodimerization. These observations highlight the importance of both protein orientation and packing density on particle behavior.

While previous work introduced the use of coiled-coil proteins to drive self-assembly of inorganic nanoparticles into larger hierarchical structures[24–26], this is the first demonstration that orientational discrimination of biomolecular recognition can control self-assembly versus colloidal stability of inorganic nanoparticles. In particular, colloidal stability has not been shown previously to be controlled by coiled-coil proteins. The tendency of cysA-Bcys conjugated GNPs to self-assemble and the colloidal stability of cysA-cysB conjugated GNPs as observed in these experiments suggest that interparticle and intraparticle coiled-coil heterodimerization is energetically favorable for these two types of GNPs, respectively, verifying the material design illustrated in Figure 1.

The cysA-Bcys conjugated GNPs could be stored in a colloidally stable state in the presence of a large excess of solubilized coiled-coils, and their aggregation could be triggered upon reduction in the concentration of solubilized coiled-coils. These might be important properties in practical applications, such as detection technologies.[5–9] Future studies may include investigation of the aggregation kinetics of cysA-Bcys conjugated GNPs as a function of nanoparticle or solubilized coiled-coil concentration. In addition, the coiled-coils presented here can be easily modified with bioactive ligands or targeting moieties for both self-assembling and stable nanoparticles, via protein engineering. Thus, this approach can be tuned to create colloidally stable or self-assembling nanoparticles while maintaining the bioactivity and targeting ability of the ligands.

In summary, we report that orientational discrimination of biomolecular recognition can be harnessed as a molecular engineering tool to control nanoparticle self-assembly and stability. We demonstrated that when a pair of heterodimerizing coiled-coils was conjugated on the nanoparticle surface, simply flipping the orientation of one of the coiled-coils led to two completely different particle properties: one driving the nanoparticles into large aggregates and the other keeping them colloidally stable.

Conflicts of interest

There are no conflicts to declare

Acknowledgements

This project was supported by funds from the National Science Foundation (NSF) Career Award DMR-1151529, University of Minnesota Institute for Engineering in Medicine, and University of Minnesota Academic Health Centers. A.S. was supported by a Biotechnology Training Grant (NIH T32GM008347) and the Institute for Molecular Virology Training Program (NIH T32 AI83196). Parts of this work were carried out in the Characterization Facility at the University of Minnesota, which receives partial support from NSF through the MRSEC program.

Notes and references

1 M. P. Nikitin, T. A. Zdobnova, S. V Lukash, O. A. Stremovskiy and S. M. Deyev, *PNAS*, 2010, **107**, 5827–5832.
2 G. Eidelshtein, M. Fattal, G. Avishai and B. Kempinski, *nanomaterials*, 2016, **6**, 1–8.
3 J. Gao, X. Huang, H. Liu, F. Zan and J. Ren, *Langmuir*, 2012, **28**, 4464–4471.
4 F. Schulz, G. T. Dahl, S. Besztejan, M. A. Schroer, F. Lehmkühler, G. Grübel, T. Vossmeyer and H. Lange, *Langmuir*, 2016, **32**, 7897–7907.
5 K. Saha, S. S. Agasti, C. Kim, X. Li and V. M. Rotello, *Chem. Rev.*, 2012, **112**, 2739–2779.
6 M. S. Draz and H. Shafiee, *Theranostics*, 2018, **8**, 1985–2017.
7 S. R. Ahmed, J. Kim, V. T. Tran, T. Suzuki, S. Neethirajan, J. Lee and E. Y. Park, *Sci. Rep.*, 2017, **7**, 1–11.
8 M. E. Hamdy, M. Del Carlo, H. A. Hussein, T. A. Salah, A. H. El-Deeb, M. M. Emara, G. Pezzoni and D. Compagnone, *J. Nanobiotechnology*, 2018, **16**, 1–12.
9 Y. S. Borghei, M. Hosseini, M. Dadmehr, S. Hosseinkhani, M. R. Ganjali and R. Sheikhnejad, *Anal. Chim. Acta*, 2016, **904**, 92–97.
10 C. M. Li, L. L. Zheng, X. X. Yang, X. Y. Wan, W. B. Wu, S. J. Zhen, Y. F. Li, L. F. Luo and C. Z. Huang, *Biomaterials*, 2016, **77**, 216–226.
11 X. Liu, H. Huang, Q. Jin and J. Ji, *Langmuir*, 2011, **27**, 5242–5251.
12 R. E. Holmlin, X. Chen, R. G. Chapman, S. Takayama and G. M. Whitesides, *Langmuir*, 2001, **17**, 2841–2850.
13 P. P. Pillai, S. Huda, B. Kowalczyk and B. A. Grzybowski, *J. Am. Chem. Soc.*, 2013, **135**, 6392–6395.
14 A. J. Keefe and S. Jiang, *Nat. Chem.*, 2012, **4**, 59–63.
15 A. Wu, W. Cheng, Z. Li, J. Jiang and E. Wang, *Talanta*, 2006, **68**, 693–699.
16 M. Sastry, A. Kumar, S. Datar, C. V Dharmadhikari and K. N. Ganesh, *Appl. Phys. Lett.*, 2001, **78**, 2943–2945.
17 J. Song, S. Park, S. Kim, K. Im and N. Park, *New J. Chem.*, 2017, **41**, 9590–9593.
18 A. Sanchez-Iglesias, M. Grzelczak, A. Thomas, B. Goris, J. Perez-Juste, S. Bals, G. Van Tendeloo, S. H. Donaldson, B. F. Chmelka, J. N. Israelachvili and L. M. Liz-Marzan, *ACS Nano*, 2012, **6**, 11059–11065.
19 Y. Ofir, B. Samanta and V. M. Rotello, *Chem. Soc. Rev.*, 2008, **37**, 1909–30.
20 B. S. Mann, W. Shenton, M. Li and S. Connolly, *Adv. Mater.*, 2000, **4**, 147–150.
21 N. L. Rosi and C. A. Mirkin, *Chem. Rev.*, 2005, **105**, 1547–1562.
22 R. C. Mucic, J. J. Storhoff, C. A. Mirkin and R. L. Letsinger, *J. Am. Chem. Soc.*, 1998, **120**, 12674–12675.
23 C. J. Loweth, W. B. Caldwell, X. Peng, A. P. Alivisatos and P. G. Schultz, *Angew. Chem. Int. Ed.*, 1999, **38**, 1808–1812.
24 M. M. Stevens, N. T. Flynn, C. Wang, D. A. Tirrell and R. Langer, *Adv. Mater.*, 2004, **16**, 915–918.

25 M. Obana, B. R. Silverman and D. A. Tirrell, *J. Am. Chem. Soc.*, 2017, **139**, 14251–14256.
26 A. P. Schoen, B. Hommersom, C. Heilshorn and M. E. Leunissen, *Soft Matter*, 2013, **9**, 6781–6785.
27 S. A. Connolly and D. J. Fitzmaurice, *Adv. Mater.*, 1999, **11**, 1202–1205.
28 W. Shenton, S. A. Davis and S. Mann, *Adv. Mater.*, 1999, **11**, 449–452.
29 W. Shen, K. Zhang, J. A. Kornfield and D. A. Tirrell, *Nat. Mater.*, 2006, **5**, 153–158.
30 B. Liu, Y. Liu, J. J. Riesberg and W. Shen, *J. Am. Chem. Soc.*, 2010, **132**, 13630–13632.
31 G. Frens, *Nat. Phys. Sci.*, 1973, **241**, 20–22.
32 S. K. Ghosh and T. Pal, *Chem. Rev.*, 2007, **107**, 4797–4862.
33 W. Haiss, N. T. K. Thanh, J. Aveyard and D. G. Fernig, *Anal. Chem.*, 2007, **79**, 4215–4221.
34 S. B. Kennedy, K. Littrell, P. Thiyagarajan, D. A. Tirrell and T. P. Russell, *Macromolecules*, 2005, **38**, 7470–7475.
35 X. Liu, M. Atwater, J. Wang and Q. Huo, *Colloids Surfaces B Biointerfaces*, 2007, **58**, 3–7.
36 J. Wei, L. Zheng, X. Lv, Y. Bi, W. Chen, W. Zhang, Y. Shi, L. Zhao, X. Sun, F. Wang, S. Cheng, J. Yan, W. Liu, X. Jiang, G. F. Gao and X. Li, *ACS Nano*, 2014, **8**, 4600–4607.
37 D. A. Urban, L. Rodriguez-Lorenzo, S. Balog, C. Kinnear, B. Rothen-Rutishauser and A. Petri-Fink, *Colloids Surfaces B Biointerfaces*, 2016, **137**, 39–49.
38 A. Boal, F. Ilhan, J. DeRouchey, T. Thurn-Albrecht, T. Russell and V. Rotello, *Nature*, 2000, **404**, 746–8.
39 S. Srivastava, A. Verma, B. L. Frankamp and V. M. Rotello, *Adv. Mater.*, 2005, **17**, 617–621.

TABLE OF CONTENTS ENTRY

Orientational discrimination of biomolecular recognition is exploited to control nanoparticle self-assembly and colloidal stability.